Electric-field gradients at ^{111}Cd in delafossite oxides ABO_2 (A=Ag, Cu; B=Al, Cr, Fe, In, Nd, Y)

R. N. Attili,* M. Uhrmacher, K. P. Lieb, and L. Ziegeler

II. Physikalisches Institut, Universität Göttingen, D-37073 Göttingen, Germany

M. Mekata

Department of Applied Physics, Fukui University, 3-9-1, Fukui 910, Japan

E. Schwarzmann

Institut für Anorganische Chemie, Universität Göttingen, D-37077 Göttingen, Germany

The electric-field gradient of ^{111}In(EC)^{111}Cd nuclei at cation sites in the delafossites $A^{+1}B^{+3}O_2$ have been measured using perturbed angular correlation spectroscopy. The radioactive ^{111}In tracers were introduced into the samples via ion implantation. The temperature dependence of the electric-field gradient of ^{111}Cd in the compounds $CuFeO_2$, $CuAlO_2$, $CuCrO_2$, and $CuYO_2$ was measured in the temperature range 14–1073 K, whereas for $AgCrO_2$, $AgInO_2$, and $CuNdO_2$ only measurements at room temperature were carried out. In each substance at least one electric-field gradient with axial symmetry was found and attributed to B sites. The scaling of this electric-field gradient with the cation-oxygen bond length is discussed and compared with predictions of the point-charge model and measurements in binary metal oxides.

I. INTRODUCTION

The perturbed γ-ray angular correlation method (PAC) has often been used to study, with the help of the hyperfine interaction of radioactive probe nuclei, the properties of solids on an atomic scale such as magnetic and structural phase transitions, chemical reactions, and defects. The electric-field gradients (EFG's) at ^{111}Cd probe nuclei on substitutional cation sites for binary metal oxides have been systematically studied in Göttingen,[1–3] including rare-earth sesquioxides,[4,5] bixbyites (M_2O_3),[6] and ternary oxides with $M_2Cu_2O_5$ structure.[7] The PAC experiments for the last two classes of compounds gave information on the local oxygen configuration in terms of the size of the cation. The great variety of delafossites, either in the ionic radii of the B elements or in the lattice parameters provides the possibility to extend these investigations, especially because the oxygen octahedra in delafossites have the same symmetry D_{3d} as one of the octahedra in the bixbyites; therefore a direct comparison with the detailed results in bixbyites[6] is possible. The particular motivation of the present work was to search for a systematic dependence of the EFG, either on the ionic size of the B^{+3} cation or on the lattice constant itself in copper- and silver-based delafossites. As the bonding is clearly more covalent[8,9] compared to bixbyite one might expect a different behavior in the delafossites compared to purely ionic compounds.

II. THE DELAFOSSITE STRUCTURE (ABO_2)

$CuFeO_2$ was the first compound known to exhibit the delafossite structure. The Fe^{+3} ions are located at the B site in the center of regularly inclined oxygen octahedra, which are connected by monovalent Cu^+ ions (on the A site) with a twofold linear coordination parallel to the c axis [Fig. 1(a)].[8] The structure belongs to the space group $R\bar{3}m$, but a polymorphic one having the space group $P6_3/mmc$ has also been

observed, which is a stacking variant of the R phase. The $R\bar{3}m$ delafossites in the hexagonal description [Fig. 1(b)] (Ref. 10) have the lattice constants a=2.8–3.8 Å and c=17–19 Å and the unit cell contains three ABO_2. For $P6_3/mmc$ the lattice constants are a=2.8–3.5 Å and c=11.2–12.3 Å and only two ABO_2 are found in the unit cell. Such a hexagonal description favors another view of the delafossite structure: instead of discussing oxygen octahedra the compound can be viewed as a sequence of planes with different ions in the order O^{-2}-Fe^{+3}-O^{-2}-Cu^+-O^{-2}-Fe^{+3}. All two-dimensional planes form triangular lattices.

Within the family $A^{+1}B^{+3}O_2$, the A sites can be Cu, Ag, Pd, and Pt and the B sites are Al, Ga, In, Sc, Y, Cr, Fe, rare earths, etc. The Cu- and Ag-based delafossites are semiconductors, while the Pd- and Pt-based ones are conductors.[11] In both kinds of compounds the conductivity is highly anisotropic.

The compounds $CuFeO_2$, $CuCrO_2$, and $AgCrO_2$ are antiferromagnetic below their respective Néel temperatures [11 and 16 K (Ref. 10), 25 K (Ref. 12), and 24 K (Ref. 13)]. The present measurements deal with the nonmagnetic phase; experiments within the antiferromagnetic phase will be discussed in a forthcoming paper.[14]

III. PAC MEASUREMENTS

In order to characterize the delafossite compounds, the time-differential perturbed angular correlation technique was used with radioactive ^{111}In probe atoms. As a detailed description of the PAC method is found in the literature,[15] we give here only a short introduction how the EFG on a lattice site can be observed.

The traceless EFG tensor V_{ij} has the three diagonal elements V_{xx}, V_{yy}, and V_{zz} arranged according to $|V_{xx}| \leq |V_{yy}| \leq |V_{zz}|$. The tensor is completely described by
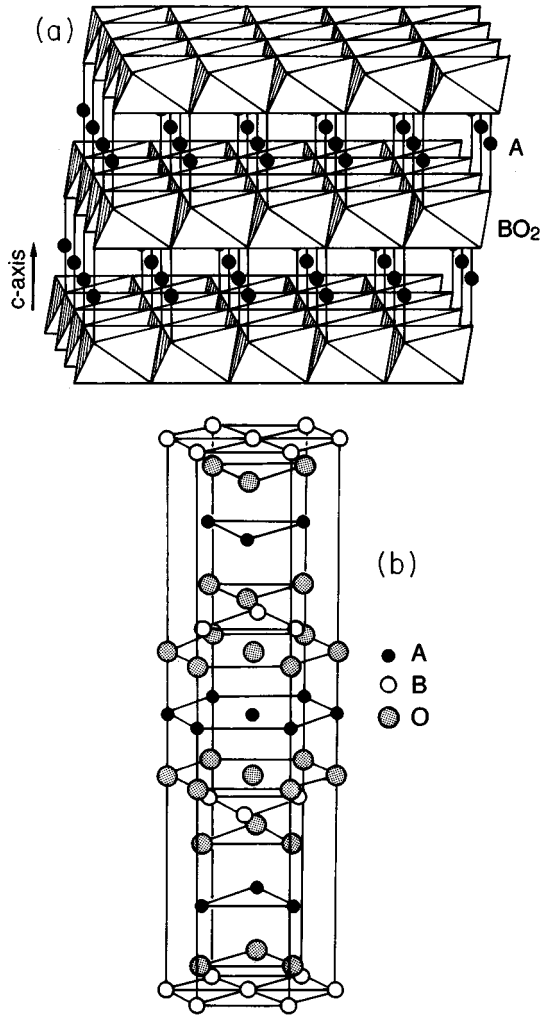
FIG. 1. (a) and (b) delafossite structure ($R\bar{3}$m).

the largest of the three components (V_{zz}) and the asymmetry parameter

$$\eta = (V_{xx} - V_{yy})/V_{zz} \qquad (1)$$

with $0 \leq \eta \leq 1$. The quadrupole constant

$$\nu_Q = (eQV_{zz})/h \qquad (2)$$

represents the strength of the EFG and η expresses the deviation of the tensor from axial symmetry ($\eta=0$).

The standard probe ^{111}In decays with a half life of $T_{1/2}=2.83$ d via electron capture to the excited $\frac{7}{2}^+$ state of ^{111}Cd. This state decays via the emission of the 171–245 keV γ-γ cascade to the $\frac{1}{2}^+$ ground state of ^{111}Cd. The intermediate level ($\frac{5}{2}^+$) is characterized by the quadrupole moment $Q=0.83$ b, the magnetic moment $\mu=-0.766\mu_N$ and the mean life $\tau=122$ ns.[16]

The samples were prepared by mixing the constituents (for example, Cu_2O and α-Fe_2O_3, in the case of $CuFeO_2$) in the correct stoichiometric ratio and heating in a controlled atmosphere. X-ray diffraction analyses were performed for all samples. In some cases the samples did not contain a single delafossite phase. Except for $CuYO_2$ (space group $P6_3/mmc$) all other compounds belong to the $R\bar{3}$m group.

Using the Göttingen ion implanter IONAS some $\approx 10^{12}$ ^{111}In$^+$ ions were implanted into the pellets at an energy of 400 keV. Then the samples were annealed under the conditions described below in order to remove radiation damage.

The PAC experiments were carried out using a conventional slow-fast setup with four NaI(Tl) detectors in 90° geometry or a fast-fast setup with four BaF$_2$ detectors positioned in the same geometry.[17] The perturbed time-differential angular correlation in polycrystalline materials is expressed by

$$W(\theta,t) = 1 + A_{22}G_{22}(t)P_2(\cos\theta), \qquad (3)$$

where θ is the angle between the detectors. A_{22} is the anisotropy coefficient of the γ-γ cascade, $P_2(\cos\theta)$ the second Legendre polynomial, and $G_{22}(t)$ the perturbation factor, containing all the information on the hyperfine interaction. In the case of static electric interaction in polycrystalline samples $G_{22}(t)$ is defined as

$$G_{22}(t) = \sum_{n=0}^{3} S_{2n}(\eta)\cos[g_{2n}(\eta)\nu_Q t]$$
$$\times \exp[-g_{2n}(\eta)\delta t]d[g_{2n}(\eta)\nu_Q t, \tau_R] \qquad (4)$$

with ν_Q being the quadrupole frequency and S_{2n} the amplitudes of the primary transition frequencies ω_n; their values are defined in Ref. 18. The parameter δ is the width of the frequency distribution. The function $d[g_{2n}(\eta)\nu_Q t, \tau_R]$ considers the damping of $G_{22}(t)$ due to the finite time resolution τ_R of the apparatus.

The twelve time spectra obtained for all possible combinations of the four detectors were used to calculate the experimental perturbation function $R(t)$ given by

$$R(t) = 2\left[\frac{W(180°,t) - W(90°,t)}{W(180°,t) + 2W(90°,t)}\right] = A_{22}\sum_{i=1}^{5} f_i G_{22}^i(t), \qquad (5)$$

where f_i are the relative fractions for different EFG's contributing to the PAC spectrum and $G_{22}^i(t)$ the corresponding perturbation factors.

IV. EXPERIMENTAL RESULTS

The various experimental EFG parameters ν_Q, δ, and η obtained in the present work are summarized in Table I. It is easily seen from the table that in most cases three fractions were found. In the following we present a detailed description of the sample treatments and EFG fractions observed.

A. CuFeO$_2$

After the ^{111}In implantation $CuFeO_2$ was annealed at 653 K for one hour in a N_2 stream. PAC measurements were performed at measuring temperatures $T_m=20$–1073 K. Some $R(t)$ functions are shown in Figs. 2(a) and 2(b). The measurements at low temperatures (20–100 K) were carried out using a closed-cycle He cryostat and the ones at high temperatures in an oven flooded with N_2. From 20 to 295 K the EFG is characterized by a unique quadrupole pattern with $\nu_{Q1}=124.6(1.1)$ MHz and $\eta_1=0$ (parameters taken at room temperature). From 423 to 1073 K this frequency slightly

TABLE I. Experimental hyperfine parameters for all the investigated compounds.

Sample	T_m (K)	f_i	ν_Q (MHz)	δ (MHz)	η	Interpretation
$CuAlO_2$		1	150.0(2.5)	2.2	0	Delafossite (B site)
	270	2	130(23)	20(6)	0.8(3)	
		3	139(3)	8.5(3.5)	0.30(7)	Al_2O_3 or $CuAl_2O_4$?
$CuCrO_2$		1	126.0(1.4)	4.7(1.5)	0	Delafossite (B site)
	295	2	131(11)	19(7)	0.3	Radiation damage?
$CuFeO_2$	295	1	124.6(1.1)	0.6	0	Delafossite (B site)
		1	131(1)	0.2	0	Delafossite (B site)
	973	2	157(6)	0.8	0	Defect?
$CuNdO_2$		1	140(4)	3.6	0	Delafossite (B site)
	295	2	89(10)	13(6)	0	?
		3	278(25)	98(27)	0	Nd_2O_3[a]
$CuYO_2$		1	136(2)	2.9(1.6)	0	Delafossite (B site)
	780	2	93.6(4.4)	6(4)	0.80(5)	
		3	151.0(3.6)	4(3)	0.20(4)	Y_2O_3[b]
$AgCrO_2$		1	131(1)	0.6	0	Delafossite (B site)
	295	2	152(15)	8	0	
		3	204(4)	3	0	Cr_2O_3[c]
$AgInO_2$		1	91(6)	4	0	Delafossite (B site)
	295	2	120(11)	(63(19)	0.5	?

[a]Reference 19.
[b]Reference 6.
[c]Reference 20.

increases to 132.1(7) MHz [see Fig. 3(a)]. At T_m=973 K a second frequency ($f_2 \approx$30%) appears with ν_{Q2}=157.3(6.1) MHz and η_2=0. After the high-temperature experiments, measurements were performed at room temperature which showed that the second frequency had disappeared. X-ray analyses of the samples before and after the PAC measurements were carried out, verifying that the compound $CuFeO_2$ had remained in the pure delafossite phase.

In the Fourier transforms of the PAC spectra, the amplitude ratio of the three primary frequencies ω_1, ω_2, and ω_3 was not typical for polycrystalline materials. Although the sample appeared to be a fine powder before the sintering procedure, it consisted of tiny flakes which showed a texture also after pressing and heating. This could be confirmed in PAC measurements by mounting the sample in two different positions (parallel and perpendicular to the detector plane), as can be seen in Fig. 2(b).

B. $CuAlO_2$

A sample of $CuAlO_2$ was annealed at 1063 K for one hour in a N_2 stream. PAC experiments at different temperatures between 12 and 710 K were performed. All spectra showed three EFG's with the following hyperfine parameters (taken at 270 K): ν_{Q1}=150.0(2.5) MHz and η_1=0; ν_{Q2}=130(23) MHz and η_2=0.8(3); ν_{Q3}=139(3) MHz and η_3=0.3(1) (Fig. 4). Only a small variation of these parameters with measuring temperature was observed [Fig. 3(b)]. In the x-ray diffraction (XRD) spectra taken before and after the PAC experiments additional phases were found, but it was not

possible to quantitatively distinguish between the Al_2O_3 or $CuAl_2O_4$ phases, because the peaks in the XRD spectra overlap.

C. $CuYO_2$

The compound $CuYO_2$ was annealed at 840 K for one hour in a N_2 stream after the ion implantation. PAC measurements, performed in the range T_m=14–780 K, showed (Fig. 4) three fractions labeled f_1, f_2, and f_3. At 780 K the highest fraction f_1 ($\approx$46%) marks the EFG with ν_{Q1}=136(2) MHz and η_1=0. The two other fractions are characterized by $f_2 \approx$31%, ν_{Q2}=93(5) MHz, and η_2=0.8(1); and $f_3 \approx$23%, ν_{Q3}=151(4) MHz, and η_3=0.2(1). Again a slight increase of the quadrupole frequency ν_{Q1} with the measuring temperature was observed [Fig. 3(c)]. The PAC results for the fractions f_2 and f_3 agree with the results found by Bartos *et al.*[6] for the Y_2O_3 phase. The hyperfine parameters concerning the Y_2O_3 phase are, due to dynamic fluctuations, very difficult to fit at low temperatures, but this fact is already known from the previous work.[6] The presence of the Y_2O_3 phase was also proven by x-ray diffraction.

D. $CuCrO_2$

Following the ^{111}In-implantation $CuCrO_2$ was submitted to an one hour annealing at 711 K in a flux of N_2; PAC measurements were performed at T_m=50–653 K. The experiments at high temperature were done under vacuum. One spectrum and its Fourier transform can be seen in Fig. 4. In all spectra of this compound, two EFG's were identified. At room temperature, fraction 1 (60%) is characterized by ν_{Q1}=126.0(1.4) MHz, η_1=0 and fraction 2 (40%) by ν_{Q2}=131(11) MHz, η_2=0.3. Nevertheless, x-ray spectra
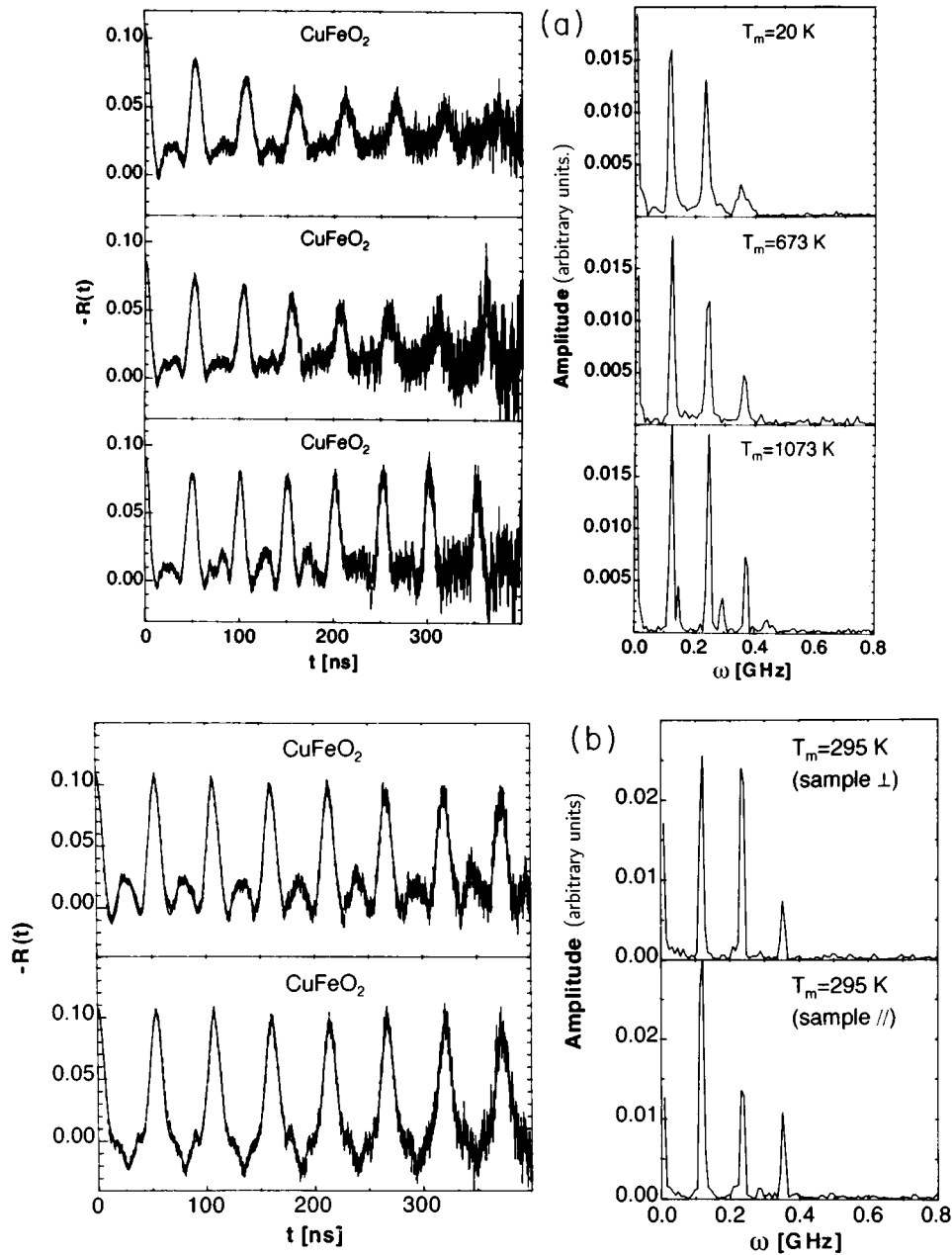
FIG. 2. (a) Perturbation functions $R(t)$ and Fourier spectra taken for ^{111}Cd in CuFeO$_2$ at different measuring temperatures T_m. (b) Perturbation functions $R(t)$ and Fourier spectra taken for ^{111}Cd in CuFeO$_2$ at room temperature with the sample perpendicular ($\perp$) and parallel ($\parallel$) to the detector plane.

taken before and after the PAC measurements verified the presence of a single delafossite phase. As in most of the delafossites, the coupling constant shows only a very weak dependence on the measuring temperature T_m [**Fig. 3(d)**].

E. CuNdO$_2$

After ^{111}In implantation into CuNdO$_2$ an isochronal annealing cycle at $T_a = 475-893$ K was performed in N_2 atmosphere. After each annealing step a PAC spectrum was taken at room temperature (Fig. 5), which was fitted with at least three EFG's: $\nu_{Q1} = 140(4)$ MHz, $\eta_1 = 0$; $\nu_{Q2} = 90(10)$ MHz, $\eta_2 = 0$, and $\nu_{Q3} = 278(25)$ MHz, $\eta_3 = 0$. The fraction 1 was attributed to the delafossite phase, the fraction 2 was not identified and the fraction 3 is due to Nd$_2$O$_3$.[19] Fraction f_1 decreases above 780 K, while f_2 and f_3 increase, possibly indicating that the compound starts to decompose. Also the

x-ray analysis of the compound after its preparation showed a complex phase mixture containing copper oxides besides CuNdO$_2$, but the typical hyperfine parameters for CuO and Cu$_2$O did not show up.[1]

F. AgCrO$_2$

As in the case of CuAlO$_2$, CuYO$_2$, and CuNdO$_2$, the AgCrO$_2$ sample did not show a single delafossite phase. In the x-ray spectrum taken before the PAC measurements, some reflexes due to silver and chromium oxides were observed; in fact the PAC spectra revealed the presence of AgCrO$_2$ and Cr$_2$O$_3$,[20] and the perturbation functions had to be fitted with three fractions. The fraction 1, attributed to the delafossite, has axial symmetry and a quadrupole frequency of $\nu_{Q1} = 131(1)$ MHz. The other two fractions have the known quadrupole coupling constants $\nu_{Q2} = 152(15)$ MHz and $\nu_{Q3} = 204(4)$ MHz and axial symmetry, typical for ^{111}Cd on substitutional cation sites in Cr$_2$O$_3$.[20] An annealing pro-
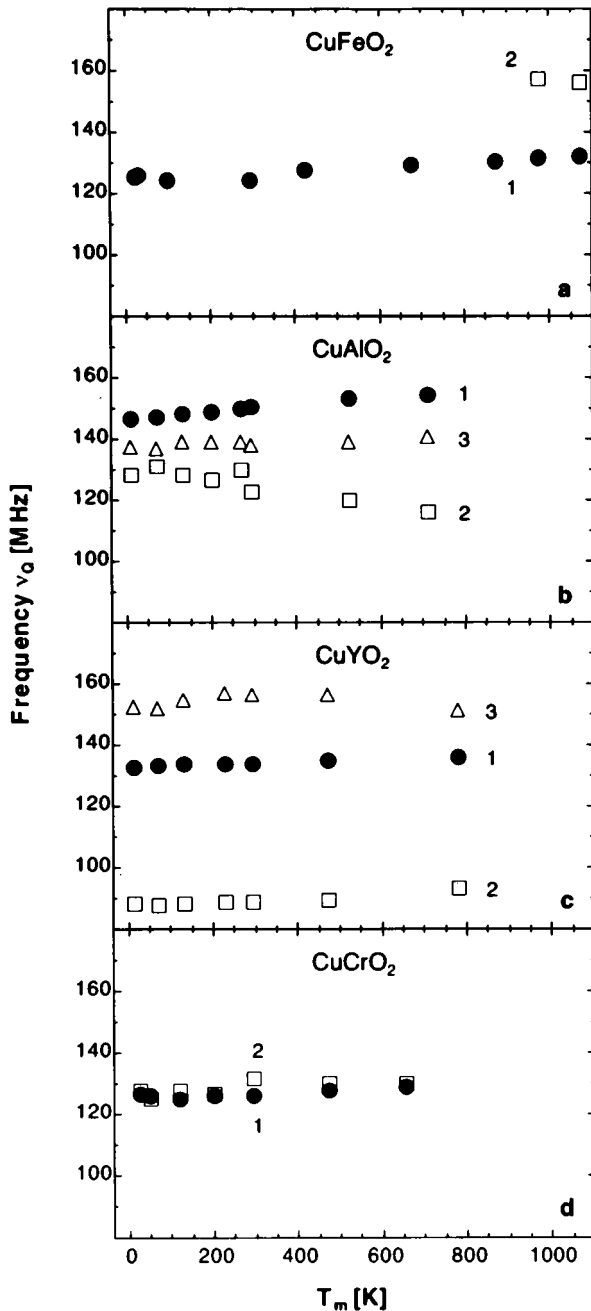
FIG. 3. Evolution of the experimental quadrupole frequencies with the measuring temperature T_m for (a) $CuFeO_2$, (b) $CuAlO_2$, (c) $CuYO_2$, and (d) $CuCrO_2$. The numbers refer to the fractions f_i listed in Table I.

gram was performed where, after each annealing step, PAC spectra were taken at room temperature (Fig. 5). If the heating was carried out during one hour in a N_2 flux, Ag^{+1} has reduced to Ag^0 and the delafossite decomposed into constituent materials. Therefore, longer annealing cycles (10 and 24 h) were performed in an oxygen stream to recover the delafossite phase as verified via x-ray and PAC spectroscopy.

G. AgInO$_2$

Tiny crystals ($\leqslant 1$ mm $\times 1$ mm) of $AgInO_2$ were produced following the procedures given in Ref. 21. X-ray analysis

showed single phase material. PAC experiments were carried out at 295 K after the sample had been annealed in air at $T_a = 473-818$ K within one hour for each step. This annealing procedure was carried out in air, carefully avoiding the decomposition temperature of 948 K.[22] Due to the small sample size, the ^{111}In implantation was difficult and only a small portion of the ^{111}In beam hit the sample, making the activity of the sample quite weak. Consequently only few measurements with low statistics could be done (Fig. 5). The PAC spectra were fitted with two EFG's: $\nu_{Q1} = 91(6)$ MHz, $\eta_1 = 0$ MHz and $\nu_{Q2} = 120(11)$ MHz, $\eta_2 = 0.5$.

V. DISCUSSION

The PAC experiments described in the previous section showed up to three EFG's for each material. In several of the delafossite compounds, the x-ray analyses revealed contaminations by additional phases, either constituent oxides or disintegration products. Using the extended knowledge on EFG's for [111]Cd in oxides, we were able to identify most foreign phases via PAC, in agreement with the XRD measurements. Some unidentified EFG's may have to be attributed to defects, but will not be further discussed in this paper. Table I contains all the observed EFG's with their interpretations. As can be seen in the table, for each compound one EFG is attributed to probes in the B site of the lattice, but no one to the A site. In the following subsections we will discuss each site assignment in detail.

A. Site allocation

1. Chemical arguments

The delafossite oxides ABO_2 have two nonequivalent cation sites in their structure. The A element with valency $+1$ is linearly coordinated by two O ions, whereas the B element with valency $+3$ occupies the center of an O octahedron. Unfortunately, from symmetry arguments of the EFG we cannot distinguish between the two sites, which both will produce an asymmetry parameter $\eta = 0$, as seen experimentally. Therefore, additional arguments are needed. Evidently, in an In-containing delafossite compound no doubts on the probe location exist. For that reason, we made much effort to measure $AgInO_2$. During their lifetime ($T_{1/2} = 2.8$ d) the [111]In^{+3} ions occupy the regular B site in that lattice. In their electron capture decay they transmute to [111]Cd^{+2} ions. The first γ quantum of the γ-γ cascade used for PAC measurements is only delayed by 110 ps. Therefore, it is reasonable to exclude the possibility of a change in the probe's position during this short period of time and during the following γ-γ cascade. However, we cannot exclude a slight distortion of the lattice caused by the larger size of the Cd^{+2} ion. If we now discuss the ^{111}In sites in the other studied delafossites we have to collect additional arguments. From a chemical point of view, the implanted trivalent ^{111}In ions should replace only the B^{+3} elements. This behavior has been already observed in some other families of oxide compounds. In the high temperature superconductivity (HTSC) precursors of cuprate structure $M_2Cu_2O_5$ with M = Sc, In, Y, Yb, Lu, Ho, and Tb,[7] the ^{111}In probes were found to substitute the M^{+3} ions, but not the Cu ions. This family is correlated to the delafossites as, at least, $Y_2Cu_2O_5$ can be reduced to $CuYO_2$. Another example is β-Ga_2O_3,[23] which has two nonequivalent lattice sites with either an octahedral or tetrahedral O coordination. Again the ^{111}In probes were found to reside on
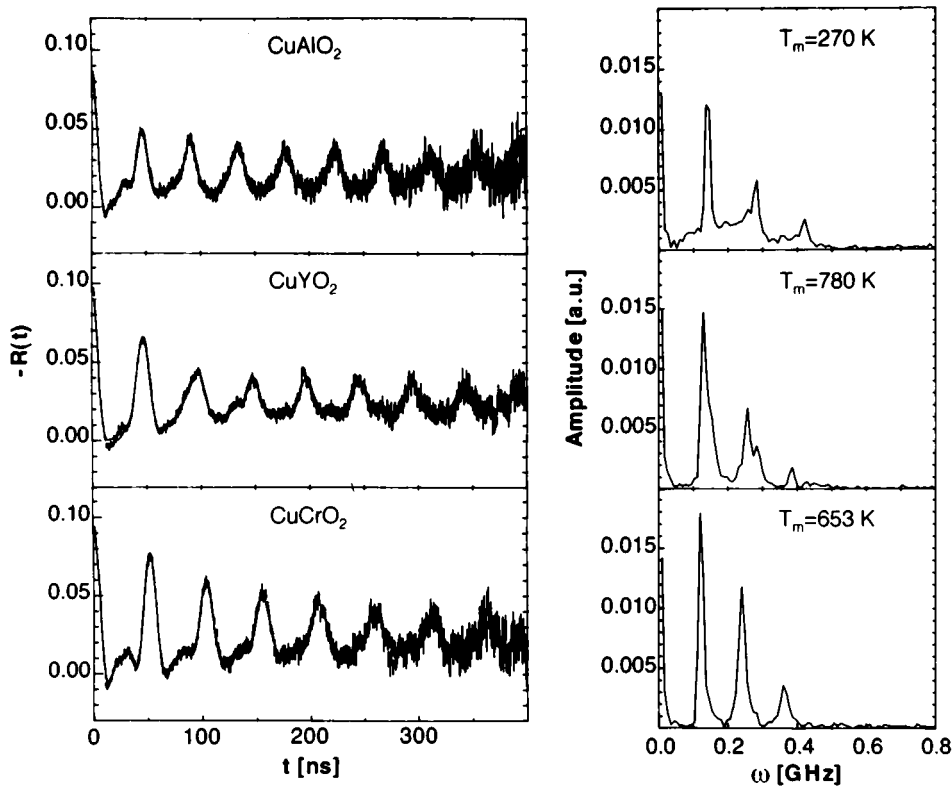
FIG. 4. Perturbation functions $R(t)$ and Fourier spectra taken for ^{111}Cd in CuAlO$_2$, CuYO$_2$, and CuCrO$_2$ at the measuring temperatures T_m indicated.
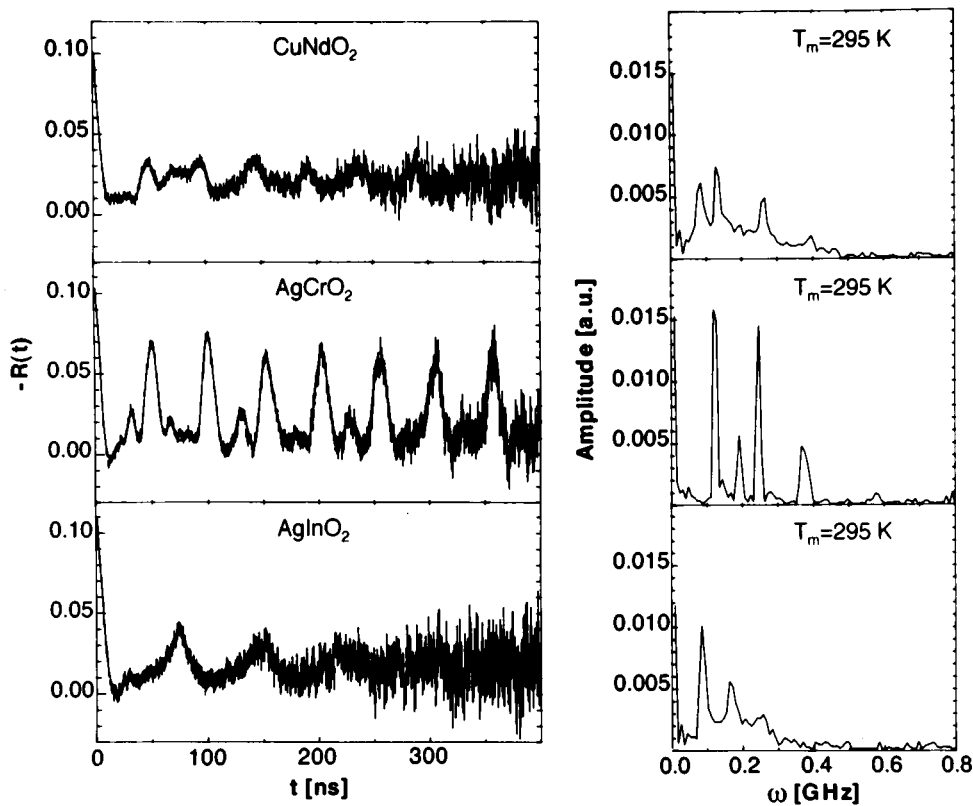
FIG. 5. Perturbation functions $R(t)$ and Fourier spectra taken for ^{111}Cd in CuNdO$_2$, AgCrO$_2$, and AgInO$_2$ at room temperature.

the octahedral sites, replacing Ga^{+3} ions. Finally, the HTSC Y-Ba-Cu-O should be mentioned; this complex oxide has many different cation sites of different valencies. Detailed PAC and electron channeling experiments concerning the lattice location of the ^{111}In probes led to the conclusion that ^{111}In ions only replace the Y^{+3} ions.[24]

2. Comparison between CEMS and PAC in CuFeO₂

Fe compounds can be analyzed by Mössbauer spectroscopy using ^{57}Fe. Conversion electron Mössbauer spectroscopy (CEMS) measurements in $CuFeO_2$ were performed at room temperature[25] to compare the EFG's of the ^{57}Fe and ^{111}Cd probes. In this measurement the B-site allocation for ^{57}Fe is evident. If the ^{111}In PAC probe replaces an Fe^{+3} ion, the lattice part (V_{zz}^{latt}) of the EFG, $V_{zz}^{latt} = V_{zz}/(1 - \gamma_\infty)$, should be the same in both experiments. At room temperature $CuFeO_2$ shows a Mössbauer absorption spectrum characterized by the quadrupole splitting $\Delta \nu = (eQV_{zz}c)/(2\hbar\omega_0) = 0.31(1)$ mm/sec and an isomer shift of 0.39(1) mm/sec.[25,26] Using the quadrupole moment of $Q = 0.082$ b[16] for the 14.4 keV state of ^{57}Fe, and the Sternheimer shielding factor $\gamma_\infty(^{57}Fe) = -9.14$,[27] we arrive at $V_{zz}^{latt} = 3.58 \times 10^{20}$ V/m^2. From the PAC measurement and using the quadrupole moment $Q(^{111}Cd) = 0.83$ b[16] and $\gamma_\infty(^{111}Cd) = -29.27$,[28] we obtain $V_{zz}^{latt} = 2.06 \times 10^{20}$ V/m^2. As both values are reasonably close, we suggest that the $^{111}Cd^{+2}$ is at the Fe site. The difference between the results may be partly due to the uncertainties of the quadrupole moments of ^{57}Fe (Refs. 16 and 29) and ^{111}Cd.

3. Antiferromagnetism in CuFeO₂, CuCrO₂, and AgCrO₂

Further support for ^{111}In occupying the B sites comes from PAC measurements in $CuFeO_2$, $CuCrO_2$, and $AgCrO_2$ below their respective Néel temperatures $T_N = 11-25$ K, in comparison with Mössbauer effect measurement in $CuFeO_2$. According to Fig. 1(b), the B-site ions are in a triangular coordination in the different layers of hexagonal structure. For the magnetic B-site ions Fe and Cr, one expects spin frustration below the Néel temperature. PAC experiments performed at 4.2 K in $CuFeO_2$ and at 15 K in $CuCrO_2$ and $AgCrO_2$ showed a slight damping of the perturbation function, consistent with a combined electric and magnetic hyperfine interaction, pointing to a very weak magnetic field of about 0.3 T. Using Mössbauer spectroscopy in $CuFeO_2$, Mekata *et al.*[10] had observed a strong magnetic field of 51.7 T at 4.2 K. The surprising results obtained with PAC may be explained by the release of spin frustration caused by the nonmagnetic solute impurity ^{111}Cd substituting a Fe cation. For details, see Ref. 14.

It is clear from the previous discussion that the available data do not allow a definitive lattice location assignment, we believe, however, that the evidence given indicates that the indium atoms are probably in B sites.

B. EFG calculations with the point charge model (PCM)

During the last years a large number of EFG's for ^{111}Cd on substitutional cation sites in metal oxides has been collected.[30] In all these compounds oxygen ions are the next neighbors of the PAC probe ^{111}In. One therefore expects that the experimental EFG is influenced by the ionic radius of the
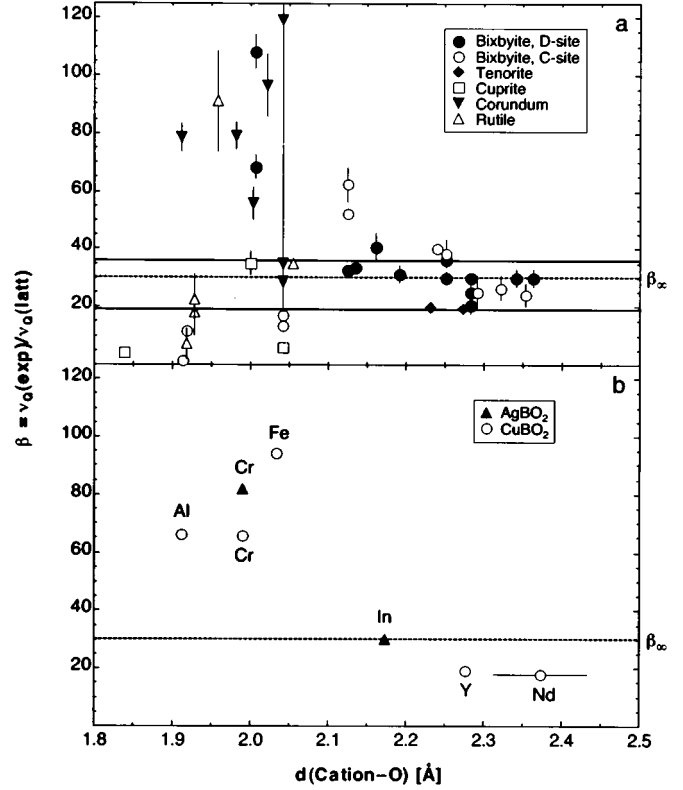
FIG. 6. Experimental shielding factor $\beta = \nu_Q(\exp)/\nu_Q^{latt}(PCM)$ versus the bond length d in oxides (a) taken from the compilation in Ref. 30 and (b) for the B site in delafossites.

cation, the lattice parameter or the distance between cation and oxygen. To test this dependence, the EFG's in oxides having the same crystallographic structure but different lattice parameters have been compared.[30] In this context the delafossites may play an important role, as they cover a distance range by far larger than all other oxide classes investigated so far.

Theoretical predictions of the EFG in oxides are difficult and rare. In most cases the unit cell is too complicated and contains too many (different) ions to perform a calculation. Furthermore band calculations may not be appropriate in these insulating or semiconducting compounds. Here we attempted to calculate the EFG using the point charge model (PCM) which is known to work reasonably well in ionic compounds. In the PCM the ions on their lattice sites are represented by their ionic charge and the EFG at the probe's site sums over all ions. As in the PCM the distortion of the probe atom's electronic shell due to the external crystal field cannot be considered in a self-consistent field calculation, it has to be accounted for by suitable shielding factors.[28,31,32] Shielding factors γ_∞ which describe the enhancement of the EFG of a charge infinitely far away, have been calculated for several probe atoms.[28] The experimental EFG is expressed as

$$V_{ij} = (1 - \gamma_\infty)V_{ij}^{latt} = \beta \cdot V_{ij}^{latt} \qquad (6)$$

if V_{ij}^{latt} is the EFG produced by the external charges.

The results of the former compilation of the EFG's in oxides by Wiarda *et al.*[30] are condensed in Fig. 6(a). The

TABLE II. PCM calculation for the A and B sites in delafossites.

Compound	A site		B site	
	ν_Q (MHz)	η	ν_Q (MHz)	η
CuAlO$_2$	889	0	69	0
CuCrO$_2$	900	0	58	0
CuFeO$_2$	923	0	40	0
CuNdO$_2$	952	0	239	0
CuYO$_2$ ($R\overline{3}$m)	955	0	200	0
CuYO$_2$ ($P6_3/mmc$)	941	0	210	0
AgCrO$_2$	664	0	48	0
AgInO$_2$	638	0	92	0

TABLE III. Distances from A and B cations to the nearest-neighbor oxygen ions in delafossites.

Compound	$d(A$-O) (Å)	$d(B$-O) (Å)	Ref.
CuAlO$_2$	1.861(1)	1.912(1)	34
CuCrO$_2$	1.85(4)	1.99(2)	35
CuFeO$_2$	1.835(8)	2.033(4)	36
CuNdO$_2$	1.8402[a]	2.3745[a]	
CuYO$_2$	1.835(12)	2.276(5)	37
AgCrO$_2$	2.07[a]	1.99[a]	
AgInO$_2$	2.076(8)	2.174(4)	21

[a]Calculated by PCM.

experimental shielding factor $\beta = \nu_Q(\exp)/\nu_Q^{\text{latt}}(\text{PCM})$ is plotted versus the average Cd-O bond length d(Cd-O). For d(Cd-O)$\geqslant$2.1 Å nearly all data are within the range $19\leqslant\beta\leqslant36$. The weighted average experimental factor $\beta\geqslant32(2)$ at these large bond lengths is in perfect agreement with the theoretical value $\beta_\infty=30.27$.[28] For smaller bond lengths the data seem to split into two branches, one with a high value around $\beta\approx85$ and the other one with values below $\beta\approx10$. The critical distance of 2.1 Å has an easy interpretation: it is just the sum of the Shannon radii[33] of O^{-2} and Cd^{+2} ions. A shorter distance is equivalent to an overlap of the electronic shells, consequently covalent bondings arise and additional contributions to the EFG have to be taken into account.[30]

To compare the measured EFG's in delafossites with PCM, calculations have been performed using the antishielding factor $\beta_\infty=-30.27$ (Ref. 28) and delafossites coordinates found in the literature. In the case of CuYO$_2$ the calculations were made for the space groups $R\overline{3}$m and $P6_3/mmc$. For CuNdO$_2$ a PCM calculation was performed using the coordinates calculated according to Ref. 9, because no values were found in the literature. Resulting ν_Q and η values for the A and B sites are given in Table II.

A fist comparison with the experimental data in Table I shows that only the AgInO$_2$ compound is correctly reproduced by the PCM. All the other PCM calculations disagree with the experiments by up to factor 3. In Ref. 30 it was proposed, that the d(Cd-O) bond length has to be larger than 2.1 Å. These bond lengths are listed in Table III and show that such condition is only fulfilled for AgInO$_2$, CuYO$_2$, and CuNdO$_2$. In fact the AgInO$_2$ compound is the only case where the PCM prediction for the B site is in agreement with the experimental result.

To test the delafossite data with the assumption of Ref. 30 we plotted in Fig. 6(b) our results (taken from Tables I, II, and III) in the same way as Fig. 6(a). We, indeed, obtained a very similar correlation between β and $d(B$-O). If we would add our data to Fig. 6(a) all points would lie on the branch with high β values at short distances. This immediately leads to two important consequences. In Fig. 6(a) data from different crystal classes are collected leaving one uncertainty: the different classes seem to favor certain regions of the plot, bixbyites are found at large bond lengths with $\beta\approx30$, whereas most of the corundum oxides show high β at short bond length. Some doubts remained whether the crystalline structure caused the variations of β or whether really the bond length is the decisive parameter. The delafossite data now solve this problem. The same lattice structure extends over the whole range of bond length. No splitting of the β branches appears, which is reasonable as in the same crystal structure the overlap of the electrons should proceed in a continuous way. A second important remark can be made. In Ref. 30 it was proposed, that covalent bonding may be the source of the additional EFG and increases β. The delafossites are known to present covalent bonding,[8,9] leading to our conclusion that, in fact, covalency is the reason which enhances or reduces the experimental shielding factor. The empirical relationship between the bond length and β summarized in Figs. 6(a) and 6(b) calls for a theoretical interpretation of EFG's in metal oxides.

VI. CONCLUSION

Using PAC the electric hyperfine interactions of ^{111}Cd impurities on substitutional sites in delafossite oxides (ABO$_2$) have been investigated. In all compounds an EFG with axial symmetry has been found which shows nearly no temperature dependence. This EFG has been attributed to probes on the substitutional B site. This conjecture is mainly based on the preference of the ^{111}In probe for a site with valency +3 and supported by low temperature PAC measurements in CuFeO$_2$, CuCrO$_2$, and AgCrO$_2$; and a CEMS measurement of CuFeO$_2$.

The strength of the experimental EFG's cannot be reproduced with the PCM, except for AgInO$_2$. But just this behavior is a new strong support for the conclusions drawn from the systematics of EFG's in many oxides presented in Ref. 30. The delafossites now directly prove that covalent bonding is responsible for the variation of the experimental enhancement factor β with the bond length.

ACKNOWLEDGMENTS

*On leave of absence: Instituto de Pesquisas Energéticas e Nucleares, IPEN-CNEN/SP, P.O. Box 11049, 05422-970 São Paulo-SP, Brazil.

[1] A. Bartos, W. Bolse, K. P. Lieb, and M. Uhrmacher, Phys. Lett. A **130**, 177 (1988).

[2] Z. Inglot, D. Wiarda, K. P. Lieb, T. Wenzel, and M. Uhrmacher, J. Phys. Condens. Matter **3**, 4569 (1991).

[3] D. Wiarda, T. Wenzel, M. Uhrmacher, and K. P. Lieb, J. Phys. Chem. Solids **53**, 1199 (1992).

[4] J. Shitu, D. Wiarda, T. Wenzel, M. Uhrmacher, K. P. Lieb, S. Bedi, and A. Bartos, Phys. Rev. B **46**, 7987 (1992).

[5] D. Lupascu, M. Uhrmacher, and K. P. Lieb, J. Phys. Condens. Matter **6**, 10 445 (1994).

[6] A. Bartos, K. P. Lieb, A. F. Pasquevich, M. Uhrmacher, and ISOLDE Collaboration, Phys. Lett. A **157**, 513 (1991).

[7] A. Bartos, M. Uhrmacher, L. Ziegeler, and K. P. Lieb, J. Alloys Compounds **179**, 307 (1992).

[8] J. P. Doumerc, A. Ammar, A. Wichainchai, M. Pouchard, and P. Hagenmuller, J. Phys. Chem. Solids **48**, 37 (1987).

[9] T. Ishiguro, N. Ishizawa, N. Mizutani, and M. Kato, J. Ceram. Soc. Jpn. **92**, 25 (1984).

[10] M. Mekata, N. Yaguchi, T. Takagi, T. Sugino, S. Mitsuda, H. Yoshizawa, N. Hosoito, and T. Shinjo, J. Phys. Soc. Jpn. **62**, 4474 (1993).

[11] D. B. Rogers, R. D. Shannon, C. T. Prewitt, and J. L. Gillson, Inorg. Chem. **10**, 723 (1971).

[12] H. Kadowski, H. Kikuchi, and A. Ajiro, J. Phys. Condens. Matter **2**, 4485 (1990).

[13] Y. Oohara, S. Mitsuda, H. Yoshizawa, N. Yaguchi, H, Kuriyama, T. Asano, and M. Mekata, J. Phys. Soc. Jpn, **63**, 847 (1994).

[14] M. Uhrmacher, R. N. Attili, K. P. Lieb, K. Winzer, and M. Mekata (unpublished).

[15] H. Frauenfelder and R. M. Steffen, *Alpha, Beta and Gamma Ray Spectroscopy* (North-Holland, Amsterdam, 1965), Vol. 2, p. 997.

[16] G. Schatz and A. Weidinger, *Nukleare Festkörper Physik* (Teubner, Stuttgart, 1992).

[17] A. Bartos, K. Schemmerling, Th. Wenzel, and M. Uhrmacher, Nucl. Instrum. Methods A **330**, 132 (1993).

[18] K. Alder, H. Albers-Schönberg, E. Heer, and T. B. Novey, Helv. Phys. Acta **26**, 761 (1953).

[19] D. Lupascu, J. Albohn, J. Shitu, A. Bartos, K. Królas, M. Uhrmacher, and K. P. Lieb, Hyperfine Interact. **80**, 959 (1993).

[20] J. Kesten, M. Uhrmacher, and K. P. Lieb, Hyperfine Interact. **59**, 309 (1990); M. Neubauer, A. Bartos, K. P. Lieb, D. Lupascu, M. Uhrmacher, and Th. Wenzel, Europhys. Lett. **29**, 175 (1995).

[21] B. U. Köhler and M. Jansen, J. Solid State Chem. **71**, 566 (1987).

[22] R. D. Shannon, D. B. Rogers, and C. T. Prewitt, Inorg. Chem. **10**, 713 (1971).

[23] A. F. Pasquevich, M. Uhrmacher, L. Ziegeler, and K. P. Lieb, Phys. Rev. B **48**, 10 052 (1993).

[24] A. Bartos and M. Uhrmacher, Phys. Rev. B **48**, 7478 (1993).

[25] P. Schaaf (unpublished).

[26] A. H. Muir Jr. and H. Wiedersich, J. Phys. Chem. Solids **28**, 65 (1967).

[27] R. M. Sternheimer, Phys. Rev. **130**, 1423 (1963).

[28] F. D. Feiock and W. R. Johnson, Phys. Rev. **187**, 39 (1969).

[29] J. O. Artman, Phys. Rev. **143**, 541 (1966).

[30] D. Wiarda, M. Uhrmacher, A. Bartos, and K. P. Lieb, J. Phys.: Condens. Matter **5**, 4111 (1993).

[31] M. H. Cohen and F. Reif, *Solid State Physics* (Academic, New York, 1957), Vol. 5, p. 322.

[32] A. Dalgarno, Adv. Phys. **11**, 281 (1962).

[33] R. D. Shannon, Acta Cryst. A **32**, 751 (1976).

[34] T. Ishiguro, A. Kitazawa, N. Mizutani, and M. Kato, J. Solid State Chem. **40**, 170 (1981).

[35] W. Dannhauser, A. P. Vaughan, J. Am. Chem. Soc. **77**, 896 (1955).

[36] C. T. Prewitt, R. D. Shannon, and D. B. Rogers, Inorg. Chem. **10**, 719 (1971).

[37] T. Ishiguro, N. Ishizawa, N. Mizutani, and M. Kato, J. Solid State Chem. **49**, 232 (1981).